

A nonequilibrium system on a restricted scale-free network

R. A. Dumer* and M. Godoy†

Instituto de Física - Universidade Federal de Mato Grosso, 78060-900, Cuiabá, Mato Grosso, Brazil.

The nonequilibrium Ising model on a restricted scale-free network has been studied with one- and two-spin flip competing dynamics employing Monte Carlo simulations. The dynamics present in the system can be defined by the probability q in which the one-spin flip process simulate the contact with a heat bath at a given temperature T , and with a probability $(1 - q)$ the two-spin flip process mimics the system subjected to an external flux of energy into it. The system network is described by a power-law degree distribution in the form $P(k) \sim k^{-\alpha}$, and the restriction is made by fixing the maximum, k_m , and minimum, k_0 , degree on distribution for the whole network size. This restriction keeps finite the second and fourth moment of degree distribution, allowing us to obtain a finite critical point for any value of α . For these critical points, we have calculated the thermodynamic quantities of the system, such as, the total m_N^F and staggered m_N^{AF} magnetizations per spin, susceptibility χ_N , and reduced fourth-order Binder cumulant U_N , for several values of lattice size N and exponent $1 \leq \alpha \leq 5$. Therefore, the phase diagram was built and a self-organization phenomena is observed from the transitions between antiferromagnetic AF to paramagnetic P , and P to ferromagnetic F phases. Using the finite-size scaling theory, we also obtained the critical exponents for the system, and a mean-field critical behavior is observed, exhibiting the same universality class of the system on the equilibrium and out of it.

I. INTRODUCTION

The dynamic evolution of equilibrium systems is related to the fact that the transition rates of its states obey the principle of microscopic reversibility. Otherwise, without the advanced tooling as proposed by Gibbs in the equilibrium scene [1], nonequilibrium systems have aroused the interest of researchers in finding out phase transitions with the particularities of continuous phase transitions of reversible systems. One kind of the nonequilibrium system is those subjected to two dynamics in competition [2, 3]. These systems are described by a master equation that involves the sum of the operators on each present process and generally each of these processes separately obeys the principle of microscopic reversibility. However, the combination of these processes may not satisfy the detailed balance and the system will be forced out of equilibrium.

In the last decades, the computerization of data acquisition on large networks, make raised the possibility of understanding the dynamical and topological stability of its networks. From that databases, the result is that large networks that span fields as diverse as the World Wide Web (WWW) or actors that have acted in a movie together, self-organize into a scale-free state [4, 5]. This means that independent of the system and its constituents, the probability $P(k)$ that a vertex interacts with k other vertices in the network, decay as a power law, i.e., $P(k) \sim k^{-\alpha}$. Barabási and Albert [5] incorporating growth and preferential attachment on its network model, were able to obtain this scale invariance, not present in the previous random [6] and small-world

networks [7]. These models and their interesting ability to describe real networks instigated the curiosity of researchers to know what would be the behavior of physical systems in complex networks [8–12]. Among these, we can highlight the simple but powerful Ising model, comprising both exact [13, 14] and computational [15–18] or approximate [19–21] results for the critical behavior on arbitrary networks.

In the same way, the study of nonequilibrium physical systems has been spreading and continuous phase transitions, characteristic of equilibrium systems is observed [22, 23]. Moreover, the same critical exponents have been obtained in reversible and irreversible systems, that is, they belong to the same universality class, acting as proof of what was conjectured by Grinstein *et al.* [24], in which says that any nonequilibrium stochastic spin system with spin-flip dynamics and up-down symmetry belongs to the same universality class. The Ising model with complex networks is already being studied with competing dynamics, analytically in 1D [25], by Monte Carlo simulations in 2D [26], and by Gaussian model in 3D [27]. However, these studies were made only for small-world networks, and by Monte Carlo simulations a mean-field critical behavior is obtained, characteristic of equilibrium systems with random interactions and convergent fourth moment of its network degree distribution [13–15, 17]. Another interesting feature of that nonequilibrium systems is the self-organization phenomena between antiferromagnetic AF to paramagnetic P , and P to ferromagnetic F phase transitions, as a function of competition parameter [2, 3, 22, 23].

With this in mind, in the present work, we have investigated the Ising model on a restricted scale-free network, where each site of the network is occupied by a spin variable that can assume values ± 1 . Divided into two sublattices, the connections between them in the network are made by the site interactions, and the degree distribution

* rafaeldumer@fisica.ufmt.br

† mgodoy@fisica.ufmt.br

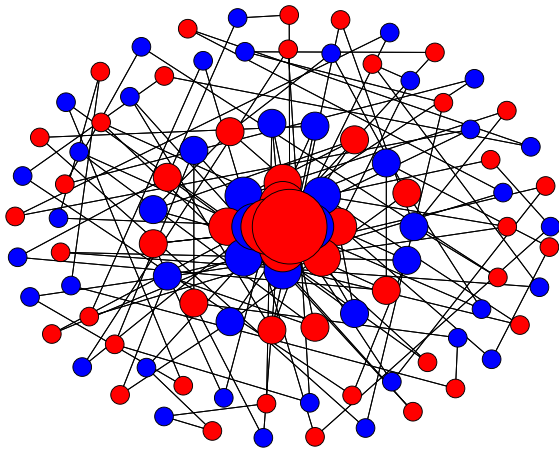


Figure 1. Schematic representation of the restricted scale-free network. Red circles indicate the sites on one of the sublattices, blue circles are the sites on the other sublattice, and the black solid lines are the connections between the two sublattices. The size of the circles is proportional to the degree of sites, varying from $k_0 = 2$ to $k_m = 8$ in the distribution with $\alpha = 3$, and $N = 10^2$.

of the network obey a power-law distribution, with fixed values of minimum and maximum degree. The system is in a nonequilibrium regime by competing between two reagent dynamic processes that do not conserve the order parameter: with competition probability q , the one-spin flip process simulates the system in contact with a heat bath at temperature T , and with probability $1 - q$, the two-spin flip process mimics the system subjected to an external flux into it. Thus, here we have investigated the phase transitions of the system and verified if the phase diagrams present the same topology of systems with these same dynamics [23, 26], and in addition, the critical exponents carrying the universality class of the system, is compared with previous works at equilibrium system [16].

This article is organized as follows: In Section II, we describe the network used and the Hamiltonian model of the system. In Section III, we present the Monte Carlo simulation method, some details concerning the simulation procedures, and the thermodynamic quantities of the system, also necessary for the application of FSS analysis. The behavior of thermodynamic quantities, phase diagrams, and critical exponents are described in Section IV. Finally, in Section V, we present our conclusions.

II. MODEL

The Ising model studied in this work has N spins $\sigma_i = \pm 1$ on a restricted scale-free network and ferromagnetic interaction of strength J_{ij} . The degree distribution on the network follows the power-law $P(k) \sim k^{-\alpha}$ and to distribute the connections between the sites, we have used the same procedures shown in the paper [16]. In order to construct a scale-free network with always convergent second and fourth moments on its degree dis-

tribution and arbitrary value of α . For that, we first define minimum k_0 and maximum k_m degree, and the exponent α of the distribution. The next procedure is to calculate the normalization constant of the distribution, $A = \sum_{k=k_0}^{k_m} k^\alpha$, and found the smaller network size that we can use and guarantee the degree distribution, $N_0 = k_m^\alpha/A$. With these values, we create a set of site numbers, $\{N_k\}$, and that will have the respective degrees k , where $N_k = AN/k^\alpha$. On that distribution of connections, we have divided the network into two sublattices, where one sublattice plays the role of central spins, while the other sublattice contains the spins in which the central spins can connect. Thus, starting with the lowest degree k_0 , connections of each N_{k_0} sites are randomly created connecting the two sublattices, and it was made until reach degree k_m and the whole set $\{N_k\}$ will be visited. An example of that construction can be seen in Fig. 1 which was chosen $\alpha = 3$, $k_0 = 2$, $k_m = 8$ and $N = 10^2$. In Fig. 1, the sites in the middle of the figure are the more connected, while the peripheral sites are the less connected, and sites from the blue sublattice are only connected with sites from the red sublattice.

Based on this construction, in the course of this work, we have selected the integer values of $1 \leq \alpha \leq 5$, $k_0 = 4$, $k_m = 10$, and network size $(32)^2 \leq N \leq (256)^2$ to study the nonequilibrium Ising model. The ferromagnetic Ising spin energy is described by the Hamiltonian on the form

$$\mathcal{H} = - \sum_{(i,j)} J_{ij} \sigma_i \sigma_j \quad (1)$$

where the sum is over all pair of spins, and J_{ij} is the ferromagnetic interaction, assuming the value of unity if sites i and j interact between the sublattices.

In the nonequilibrium system presented here, let $p(\{\sigma\}, t)$ be the probability of finding the system in the state $\{\sigma\} = \{\sigma_1, \dots, \sigma_i, \dots, \sigma_j, \dots, \sigma_N\}$ at time t , the motion equation for the probability of states evolves in time according to the master equation

$$\frac{d}{dt} p(\{\sigma\}, t) = qG + (1 - q)D, \quad (2)$$

where qG represents the one-spin flip process, relaxing the spins in contact with a heat bath at temperature T , favoring the lowest energy state of the system, and has probability q to occur. On the other hand, the $(1 - q)D$ denotes the two-spin flip process, in which the energy of the system increases by one external flow of energy into it, and has a probability $(1 - q)$ to occur. G and D are described as follows:

$$G = \sum_{i, \{\sigma'\}} [W(\sigma_i \rightarrow \sigma'_i) p(\{\sigma\}, t) - W(\sigma'_i \rightarrow \sigma_i) p(\{\sigma'\}, t)] \quad (3)$$

$$D = \sum_{i,j, \{\sigma'\}} [W(\sigma_i \sigma_j \rightarrow \sigma'_i \sigma'_j) p(\{\sigma\}, t) - W(\sigma'_i \sigma'_j \rightarrow \sigma_i \sigma_j) p(\{\sigma'\}, t)] \quad (4)$$

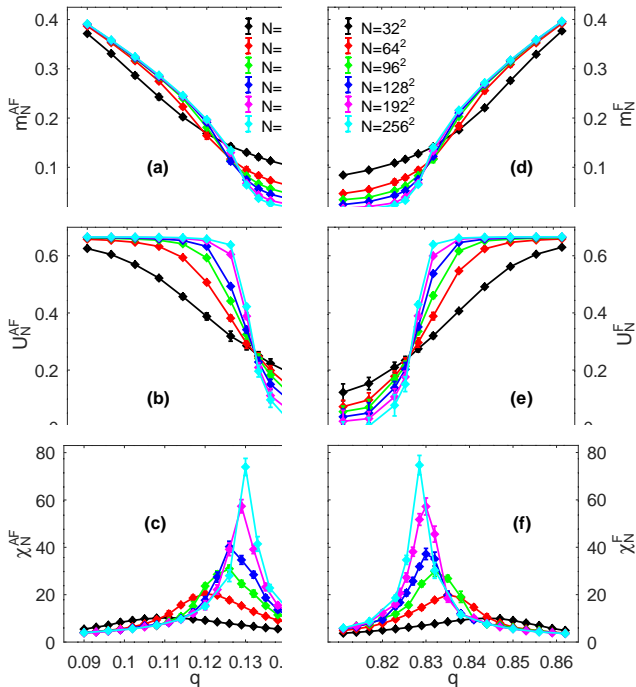


Figure 2. Behavior of the thermodynamic quantities m_L , U_L , and χ_L as a function of q for different network sizes as presented in the figures. In the $AF - P$ transition: (a) m_L^{AF} , (b) U_L^{AF} , and (c) χ_L^{AF} curves. In the $F - P$ transition: (d) m_L^{F} , (e) U_L^{F} , and (f) χ_L^{F} curves. Here, we have fixed values of $\alpha = 1$, $k_0 = 4$, $k_m = 10$, $T = 1$.

where $\{\sigma'\}$ is the spin configuration after spin flipping, $W(\sigma_i \rightarrow \sigma'_i)$ is the transition rate between the states in the one-spin flip process, and $W(\sigma_i\sigma_j \rightarrow \sigma'_i\sigma'_j)$ the transition rate between the states in the two-spin flip process.

III. MONTE CARLO SIMULATIONS

In the simulation of the system specified by the Hamiltonian in Eq. (1), we always have chosen the initial state of the system with all spin states at random, and a new configuration is generated by the following Markov process: for a given temperature T , competition probability q , distribution exponent α , network size N , and minimum k_0 and maximum k_m degree, we choose at random a spin σ_i in network, and generate a random number ξ between zero and one. If $\xi \leq q$, we choose the one-spin flip process, in which the flipping probability is dependent of $W(\sigma_i \rightarrow \sigma'_i)$ and given by the Metropolis prescription:

$$W(\sigma_i \rightarrow \sigma'_i) = \begin{cases} e^{(-\Delta E_i/k_B T)} & \text{if } \Delta E_i > 0 \\ 1 & \text{if } \Delta E_i \leq 0 \end{cases}, \quad (5)$$

where ΔE_i is the change in energy after flipping the spin, $\sigma_i \rightarrow \sigma'_i$, k_B is the Boltzmann constant, and T the temperature of the system. Thus, the acceptance of a new

state is guaranteed if $\Delta E_i \leq 0$, but, in the case where $\Delta E > 0$ the acceptance is pondered by the probability $\exp(-\Delta E_i/k_B T)$ and just guaranteed if by choosing a random number, $0 < \xi_1 < 1$, it is $\xi_1 \leq \exp(-\Delta E_i/k_B T)$. On the other hand, if none of these conditions are satisfied, we do not change the state of the system. Now, if $\xi > q$ the two-spin flip process is chosen, and in addition to the spin σ_i we also randomly choose one of its neighbors σ_j , and these two spins are flipping simultaneously according to transition rate $W(\sigma_i\sigma_j \rightarrow \sigma'_i\sigma'_j)$ given by

$$W(\sigma_i\sigma_j \rightarrow \sigma'_i\sigma'_j) = \begin{cases} 0 & \text{if } \Delta E_{ij} \leq 0 \\ 1 & \text{if } \Delta E_{ij} > 0 \end{cases}, \quad (6)$$

where ΔE_{ij} is the change in the energy after flipping the spins σ_i and σ_j , and consequently, in this process, the new state is only accepted if $\Delta E_{ij} > 0$.

Repeating the Markov process N times, we have one Monte Carlo Step (MCS). In our simulations, we have waited for 10^4 MCS to the system reach the stationary state, in the whole the network sizes and adjustable parameters. In order to calculate the thermal averages of the interest quantities, we used more 4×10^4 MCS, and the average over samples was done using 10 independent samples for any configuration.

The measured thermodynamic quantities in our simulations are: magnetization per spin m_N^{F} , staggered magnetization per spin m_N^{AF} , magnetic susceptibility χ_N and reduced fourth-order Binder cumulant U_N :

$$m_N^{\text{F}} = \frac{1}{N} \left[\left\langle \sum_{i=1}^N \sigma_i \right\rangle \right], \quad (7)$$

$$m_N^{\text{AF}} = \frac{1}{N} \left[\left\langle \sum_{i=1}^N (-1)^{(r+c)} \sigma_i \right\rangle \right], \quad (8)$$

$$\chi_N = \frac{N}{k_B T} \left[\langle m^2 \rangle - \langle m \rangle^2 \right], \quad (9)$$

$$U_N = 1 - \frac{[\langle m^4 \rangle]}{3 [\langle m^2 \rangle]^2}, \quad (10)$$

where $[\dots]$ representing the average over the samples, and $\langle \dots \rangle$ the thermal average over the MCS in the stationary state. To facilitate the calculation of m_N^{AF} , the sites on the network are labeled as if we had a square lattice, $N = L^2$, in this way, r and c are the row and column of the site i , respectively. In Eqs. (9) and (10), m can be used to represent m_N^{F} or m_N^{AF} .

In the vicinity of the stationary critical point λ_c , the Eqs. (7), (8), (9) and (10) obey the following finite-size scaling relations [28]:

$$m_N = N^{-\beta/\nu} m_0(N^{1/\nu} \epsilon), \quad (11)$$

$$\chi_N = N^{\gamma/\nu} \chi_0(N^{1/\nu} \epsilon), \quad (12)$$

$$U'_N = N^{1/\nu} \frac{U'_0(N^{1/\nu} \epsilon)}{\lambda_c}, \quad (13)$$

where $\epsilon = (\lambda - \lambda_c)/\lambda_c$ (λ and λ_c can be used T or q), and β , γ and ν are the critical exponents related the magnetization, susceptibility and length correlation, respectively. The functions $m_0(N^{1/\nu} \epsilon)$, $\chi_0(N^{1/\nu} \epsilon)$ and $U_0(N^{1/\nu} \epsilon)$ are the scaling functions.

Using the data from simulations for the network sizes $(32)^2 \leq N \leq (256)^2$ in the Eqs. (11), (12) and (13), we have obtained the critical exponents ratio β/ν , γ/ν , and ν^{-1} from the slope of the straight lines in the log-log plot of $m_N(\lambda_c)$, $\chi_N(\lambda_c)$, and $U'_N(\lambda_c)$ (derivative of U_N) as a function of N . Besides that, we also used data collapse from scaling functions to estimate the critical exponent values.

IV. RESULTS

In this section, we present and discuss the results of the nonequilibrium Ising model on a restricted scale-free network. For the two dynamic processes, we have an adjustable parameter q that controls the dynamic competition in the system. If $0 < q < 1$, the two dynamic processes have a non-null probability to be chosen and acting in the system, making it irreversible with respect to the temporal evolution of its states. As these processes favor the states of higher and lower energy of the system, with the competition is possible to find stationary states in the AF , F , and P phases, based on the Hamiltonian of the system, Eq. (1). With this, it is worth noting that to obtain a self-organization phenomenon passing from a F to P and from P to AF phases, the division of the network into two sublattices is essential, once that for nonfrustrated antiparallelism we must to have well-defined who the central spins are, and to whom they can connect in the network.

Therefore, the first results can be seen in Fig. 2, where we have displayed the thermodynamic quantities obtained with Eqs. (7), (8), (9) and (10). These quantities were calculated as a function of the competition parameter q , in which is verified that for lower values of q we found an AF phase, and for higher values of q , an F phase is observed. These phases are easily explained when we look at the dynamics, once that for lower values of q , the two-spin flip mechanism prevails and this favors the state of high energy in the system, which based on the ferromagnetic Ising model Hamiltonian is the one where

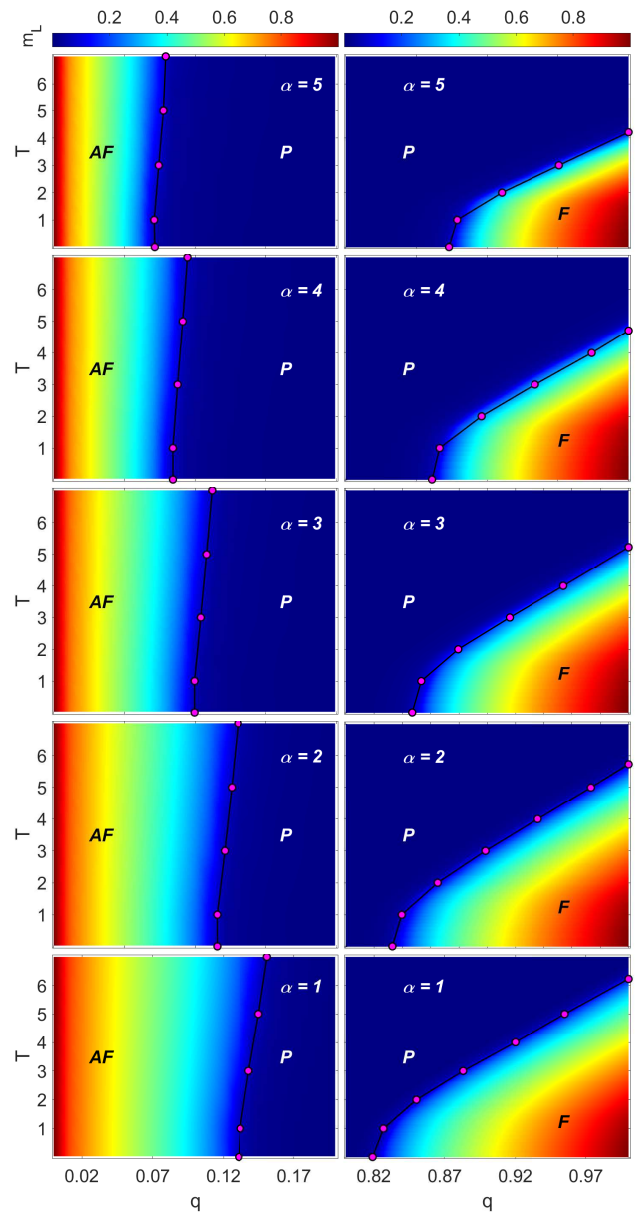


Figure 3. Phase diagrams in the plane temperature T versus q for some values of the exponent α and fixed values of $k_0 = 4$ and $k_m = 10$. On the top, we have the color bar of m_L where the left side represent the staggered magnetization m_N^{AF} illustrating the $AF - P$ transition and the right side the magnetization per spin m_N^F illustrating the $F - P$ transition. The magenta circles are the critical points estimated by the crossing of U_L curves and the black solid lines are just a guide for the eyes indicating the phase transition lines.

the spin states are antiparallel, i. e., AF phase. This AF phase is made explicit in Fig. 2(a) with the m_N^{AF} curves, and with this magnetization is calculated U_N^{AF} present in Fig. 2(b), and its susceptibility χ_N^{AF} in Fig. 2(c). On the other hand, for higher values of q , the one-spin flip mechanism prevails, and as it favors the states of lower energy in the system, i.e., all spins in the same state, an ordered phase is also observed, F phase. The quantities

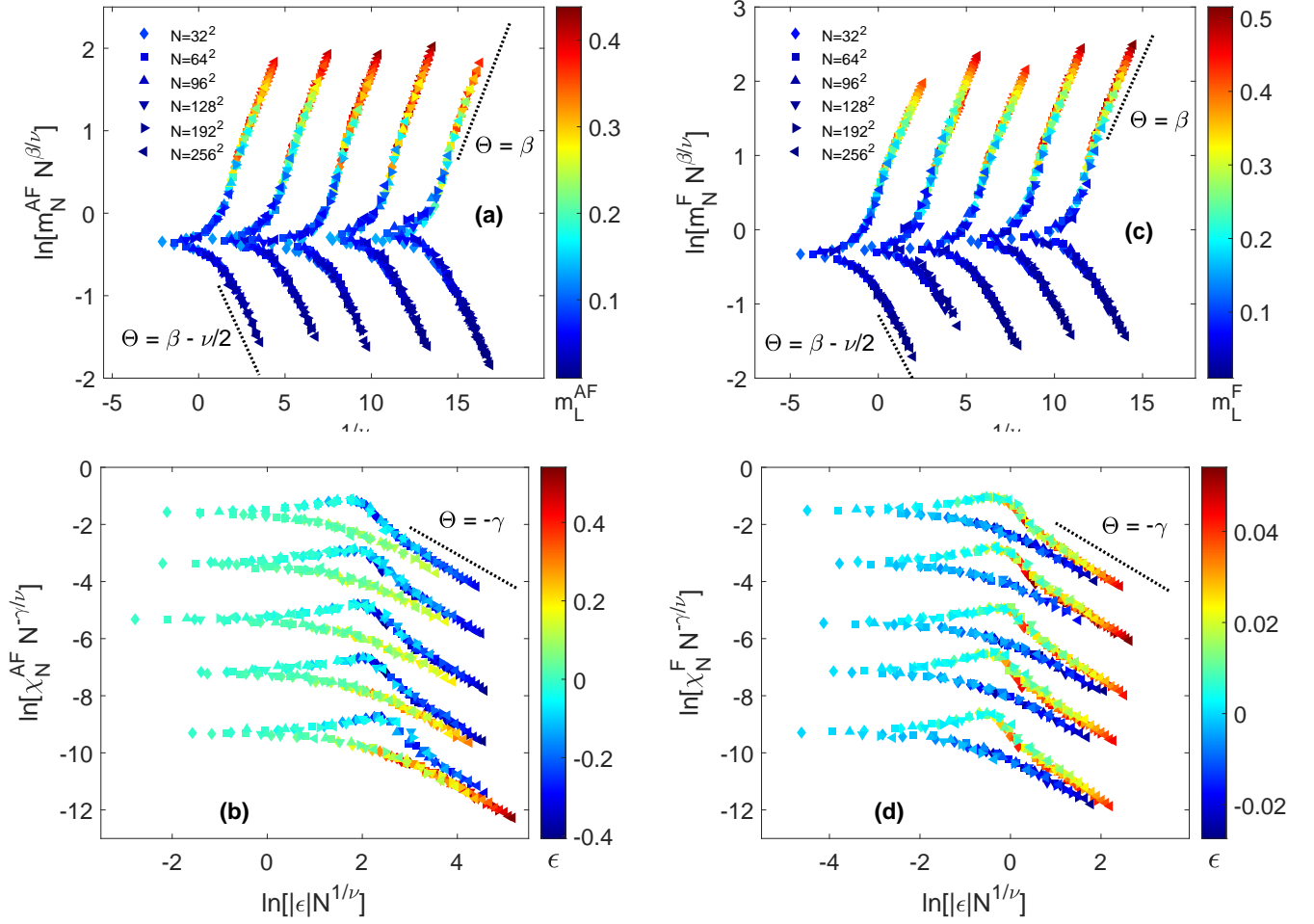


Figure 4. Data collapse of m_L^{AF} (a), χ_L^{AF} (b), m_L^F (c) and χ_L^F (d) for different network sizes as presented in the figures. In (a) and (c) from the left to the right side we have respectively $\alpha = 1, 2, 3, 4$ and 5 , and m_L^{AF} and m_L^F color bars as shown in the figures. In (b) and (d), with $\epsilon = (q - q_c)/q_c$ color bar and from the top to bottom we have the collapses with $\alpha = 1, 2, 3, 4$ and 5 , respectively. In these figures, we have changed the positions curves for $1 < \alpha \leq 5$ in order to compare all the collapses obtained. The critical exponents and critical points used here can be seen in Table I and Table II respectively. Here, we have fixed $T = 1$, $k_0 = 4$, $k_m = 10$.

related to this phase is specifically the magnetization m_N^F curves in Fig. 2(d), and the U_N^F and χ_N^F curves in Figs. 2(e) and 2(f), respectively.

We have used the curves of the fourth-order Binder cumulants for different network sizes to identify the critical points and order phase transition [29–32]. The intersection point of the U_N curves indicates the phase transition point on a second-order phase transition. With the critical point in hand for several values of adjustable parameters, a phase diagram was built, which can be seen in Fig. 3. Therefore, for these diagrams and later results, we will limit the values $k_0 = 4$ and $k_m = 10$, once we can build all networks with sizes $(32)^2 \leq N \leq (256)^2$, integer exponent $1 \leq \alpha \leq 5$, and compare with others equilibrium [13, 14, 16] and nonequilibrium [23, 26] Ising model results. Fig. 3 presents the phase diagrams of temperature T as a function of competition parameter q for some values of α , in which we can see the AF , F , and P phases.

In these diagrams (Fig. 3), we have illustrated the self-organization phenomena with the transitions between AF to P phases, and P to F phases. Since the scale is fixed in all the figures, we can also see that when we decrease the value of α , the region of ordered phases, F and AF , increases. This change in the topology of the diagram is related to the degree distribution, once the lower values of exponent α mean a high probability of having more connected sites on network, i.e., more sites with a degree k_m . Consequently, knowing that more connected sites on the stationary ordered state require more energy to override its interactions, larger are the regions of the ordered phases. Another interesting observation that we can do, is regarding the shape of the regions in the ordered phases. The ferromagnetic phases are driven by the one-spin flip mechanism described by Metropolis prescription, which is very dependent on T , and for high T we observe the disordered phase P . On the other hand, AF phases is driven by the two-spin flip mecha-

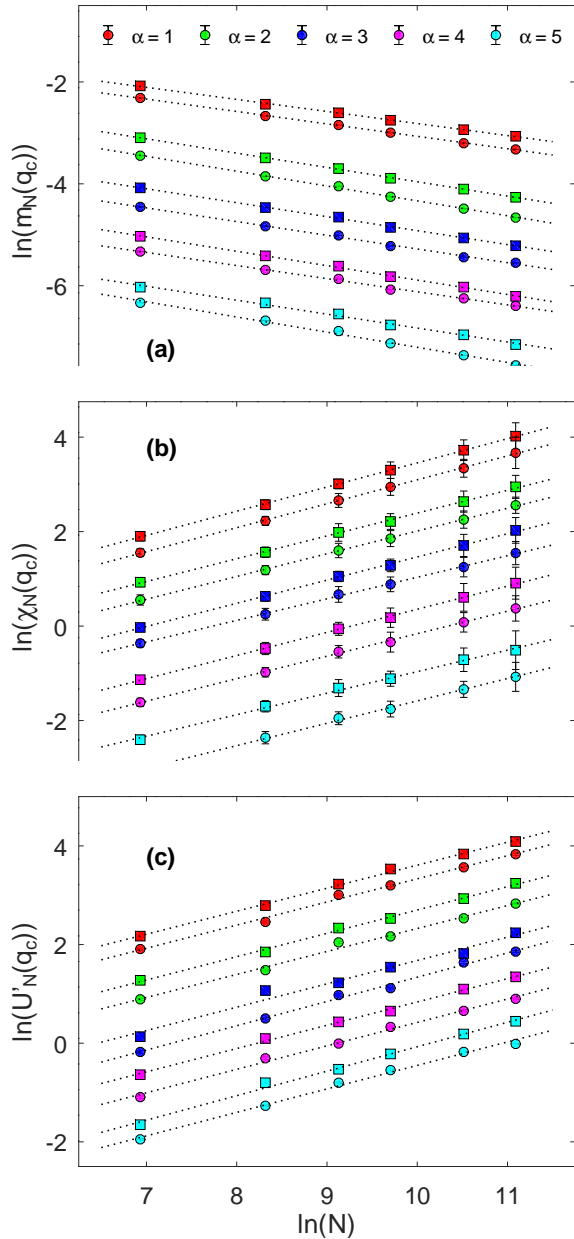


Figure 5. In log-log plots is presented linear fits (black dotted lines) of thermodynamic quantities in the critical point, m_L^{AF} (\square) and m_L^{F} (\circ) in (a), χ_L^{AF} (\square) and χ_L^{F} (\circ) in (b), and U_L^{AF} (\square) and U_L^{F} (\circ) in (c), both as a function of the network size N , and different values of α as shown in the figures. Here we have fixed $T = 1$, $k_0 = 4$ and $k_m = 10$. The critical points used for these fits can be seen in Table II.

nism, in which is a simpler process and little influenced by temperature.

All systems belonging to a given universality class share the same set of critical exponents. The critical points can be used to describe the critical behavior in the sense of universality class with the set of critical exponents. Here, we have computed the exponents β , γ and ν , by two methods. The first one is based on the data

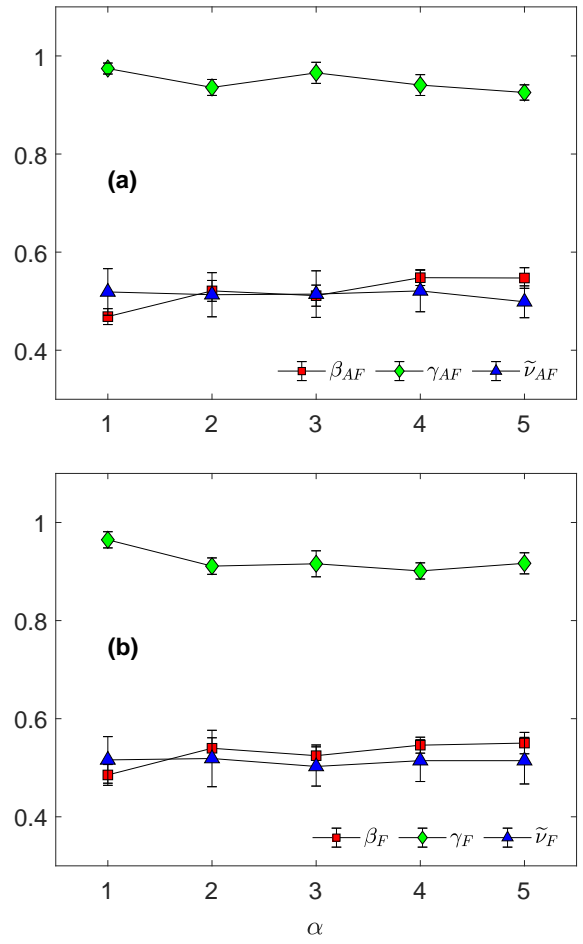


Figure 6. Average static critical exponents β , γ , and ν , obtained from the slope of scaling functions and the data collapse of magnetization and susceptibility curves as a function of α . (a) For $AF-P$ transition and (b) for the $F-p$ transition. These exponents were obtained with fixed values of $T = 1$, $k_0 = 4$ and $k_m = 10$.

collapse, in which we use the scaling relations, Eqs. (11) and (12), to obtain the scaling functions of magnetization and susceptibility with its collapsed curves. This is possible because in the proximity of the critical points the scaling relations are independent of network size with the correct critical exponents and critical point of the system [29–31]. To obtain the critical exponents by this method and using the already estimated critical points, we have plotted the scaling functions $m_0(N^{1/\nu}\epsilon)$ and $\chi_0(N^{1/\nu}\epsilon)$ as a function of $|\epsilon|N^{1/\nu}$ for different network sizes and in the proximity of critical points. Therefore, for $\epsilon \rightarrow 0$ and adjusting the involved critical exponents, when the curves of different network sizes collapse better into a single curve, these exponents used are considered the critical exponents of the system.

Fig. 4 display the scaling functions $m_0(N^{1/\nu}\epsilon)$ and $\chi_0(N^{1/\nu}\epsilon)$ collapsed in the log-log plot to obtain its asymptotic behavior. In these figures, we have fixed $T = 1$ to obtain the critical exponents of the system both in the $F-P$ transition and in the $AF-P$ tran-

α	β_F	γ_F	$\nu_F (m_L)$	$\nu_F (\chi_L)$	β_{AF}	γ_{AF}	$\nu_{AF} (m_L)$	$\nu_{AF} (\chi_L)$
1	0.51 ± 0.04	0.98 ± 0.03	1.98 ± 0.03	2.02 ± 0.04	0.50 ± 0.03	1.00 ± 0.02	2.00 ± 0.04	2.00 ± 0.03
2	0.54 ± 0.04	0.92 ± 0.03	2.00 ± 0.05	2.00 ± 0.04	0.51 ± 0.04	0.95 ± 0.03	2.00 ± 0.05	2.00 ± 0.03
3	0.52 ± 0.04	0.93 ± 0.05	2.00 ± 0.02	1.96 ± 0.02	0.50 ± 0.04	1.00 ± 0.04	2.00 ± 0.03	2.02 ± 0.04
4	0.56 ± 0.03	0.90 ± 0.03	1.96 ± 0.03	2.06 ± 0.04	0.56 ± 0.03	0.96 ± 0.04	2.02 ± 0.04	2.04 ± 0.03
5	0.54 ± 0.04	0.95 ± 0.04	1.96 ± 0.04	2.06 ± 0.03	0.55 ± 0.04	0.95 ± 0.03	2.01 ± 0.02	1.92 ± 0.03

Table I. Critical exponents obtained by the data collapse method for several values α . The $F - P$ transitions are denoted by F subscript and the $AF - P$ transitions are denoted by AF subscript. In these transitions, the data collapse of magnetization and susceptibility curves returns us respectively $\nu(m_L)$ and $\nu(\chi_L)$ estimates using the ν exponent. For these exponents, we have fixed $T = 1$ and $k_0 = 4$ and $k_m = 10$. The collapsed curves can be seen in Fig. 4.

sition, for all values of α . In Fig. 4(a), we can see the function $m_0(N^{1/\nu}\epsilon)$ in the log-log plot, produced with the collapse of m_N^{AF} curves, and with this was obtained the exponents β and ν . In the same way, in Fig. 4(b) the scaling function $\chi_0(N^{1/\nu}\epsilon)$ is presented in the log-log plot with χ_N curves based on staggered magnetization, in which with the best data collapse we have obtained the exponent γ , and another estimated value for the ν exponent. On the other hand, in the $F - P$ transition, Figs. 4(c) and 4(d), respectively, contain the log-log plot of the scaling functions based on m_N^F and its susceptibility, χ_N^F . The asymptotic behavior, away from the critical point of these functions, is predicted to a slope Θ related to the obtained critical exponents, once that for the magnetization curves starting from the ordered phase, below from the critical point $\Theta = \beta$, and above it $\Theta = \nu/2 - \beta$, and for the susceptibility curves we only have $\Theta = -\gamma$. The critical exponents obtained by this first method are presented in Table I and the critical point used for them can be seen in Table II.

Now, let use a second method to calculate the critical exponents and also using the scaling relations, but, with the log-log plot of m_N^{AF} and m_N^F at its respective χ_N and U_N in the proximity of the critical point as a function of N . The slope on this set of point returns us specific ratios between the critical exponents. Fig. 5(a) shown the points of m_N^{AF} and m_N^F in the vicinity of the critical point as a function of network sizes N . With the best fit of these points and its slope based on the scaling relation of Eq. (11), gives us the estimate of the ratio $-\beta/\nu$. In the same way, but for the susceptibility of these magnetizations, on the vicinity of the critical point as a function of N in the log-log plot, is presented in Fig. 5(b). The best fit with the points in this figure gives us the slope related to the ratio γ/ν presented in the scaling relation of Eq. (12). The ratio between these critical exponents is interesting but does not reveal the correct value of the exponents separately. Thus, to solve this, we used the scaling relation in Eq. (13), in which the derivative of U_N in the vicinity of the critical point and different network sizes gives us the ratio $1/\nu$. This ratio is illustrated in Fig. 5(c) by its log-log plot. All the ratio between the critical exponents obtained on this method can be found in Table II.

From these two used methods are obtained equivalent

exponents. But, we have to pay attention that as we are dealing with random interactions on the network, we do not have a well-defined dimension, and consequently, it was necessary to use scaling relations dependent only of the system size, Eqs. (11), (12) and (13). Therefore, the expected mean-field finite-size scaling exponents due to these equations are $\beta = 1/2$, $\gamma = 1$, and $\nu = 2$ [28]. If compared to the usual Ising model mean-field exponents $\beta = \tilde{\nu} = 1/2$, and $\gamma = 1$, the only exponent affected by the dimension of the system is the related to the correlation length, ν , but, can be derived by the relation $\nu = d_u \tilde{\nu}$, where d_u is the upper critical dimension, that in the Ising model is $d_u = 4$. With these information, we have computed $\tilde{\nu}$ based on the exponents ν obtained here. The critical exponents of the system, obtained by the two methods are compiled in Fig. 6(a) for $AF - P$ transitions, and in Fig. 6(b) for $F - P$ transitions, both as a function of α . Comparing these obtained critical exponents with the mean-field critical exponents, we can see that for $\alpha = 1$ is obtained the more accurate mean-field critical exponents, however, as α increase, the critical exponents are still of mean-field but with a little deviation. This deviation was explained in the work with the equilibrium Ising model on a restricted scale-free network [16], and is due to the increase of degree-degree correlations [33] with the decreasing of more connected sites.

For the sake of curiosity, our network was labeled as a square lattice, which we always use $N = L^2$ sites. Thus, changing N in Eqs. (11), (12) and (13) by L , we have the scaling relations depending on the dimension of the system, that in our case is two dimensions. With these new scaling relations, we have computed again the critical exponents of the system and we have obtained the same critical exponents of systems upper the Ising model critical dimension, by adding long-range interactions on a regular square lattice [15, 26]. It indicates that with our selected network sizes $N = L^2$, we also could use the scaling relations depending on the dimension of the system to calculate the critical exponents. However, when dealing with complex networks, this dimensioning possibility is not always available, once that the objective is to model real networks [12, 34, 35]. In this case, Hong *et al.* [28] proposed scaling relations for complex networks independent of system dimension, and from them, obtained the set of mean-field finite-size-scaling exponents.

α	q_c^F	q_c^{AF}	$(-\beta/\nu)_F$	$(\gamma/\nu)_F$	$(1/\nu)_F$	$(-\beta/\nu)_{AF}$	$(\gamma/\nu)_{AF}$	$(1/\nu)_{AF}$
1	0.8267 ± 0.0002	0.1320 ± 0.0002	0.24 ± 0.04	0.51 ± 0.05	0.47 ± 0.06	0.24 ± 0.04	0.51 ± 0.04	0.47 ± 0.06
2	0.8396 ± 0.0003	0.1156 ± 0.0002	0.28 ± 0.04	0.48 ± 0.05	0.47 ± 0.07	0.29 ± 0.05	0.48 ± 0.05	0.47 ± 0.05
3	0.8534 ± 0.0004	0.0995 ± 0.0005	0.27 ± 0.06	0.49 ± 0.05	0.47 ± 0.06	0.27 ± 0.05	0.46 ± 0.05	0.49 ± 0.06
4	0.8664 ± 0.0004	0.0842 ± 0.0004	0.28 ± 0.05	0.49 ± 0.06	0.47 ± 0.05	0.26 ± 0.04	0.48 ± 0.05	0.48 ± 0.05
5	0.8788 ± 0.0004	0.0714 ± 0.0004	0.27 ± 0.06	0.46 ± 0.05	0.50 ± 0.06	0.30 ± 0.05	0.47 ± 0.03	0.48 ± 0.04

Table II. Critical points obtained by the intersection of U_L curves, and the critical exponents by the second method for several values α . The $F - P$ transitions are denoted by F subscript and the $AF - P$ transitions are denoted by AF subscript. The slope of the straight lines are presented in Fig. 5.

V. CONCLUSIONS

Here, we have employed Monte Carlo simulations to study the thermodynamic quantities and the critical behavior of the nonequilibrium Ising model on a restricted scale-free network. By using one- and two-spin flip competing dynamics, we reach the stationary state of the system at the nonequilibrium regime. Fixing the maximum and minimum degree values for the whole network size and by using FSS analysis, we are able to always find a finite critical point even being in a network with power-law degree distribution, since we always have second and fourth convergent moments based on its distribution $P(k)$. As a result, we have obtained the critical points from the second-order phase transitions based on the intersection of U_N curves and built a phase diagram of temperature T as a function of the competition parameter q . In these diagrams, we have verified the self-organization phenomena in the transitions from AF to P phases in lower values of q , and from P to F phases in higher values of q and lower T . Because we

are dealing with a power-law degree distribution on the network, $P(k) \sim k^{-\alpha}$, decreasing the value of α , increase the number of more connected sites, and as consequence, also increase the region of the ordered phases in the diagram. Topologies equivalent to these diagrams were also obtained in previous works with the same dynamics, but in different networks and models [23, 26]. Through FSS arguments, we calculated the critical exponents β , γ , and ν for the system, and as a function of α , because we have a restricted scale-free network in which its second and fourth moments of degree distribution are convergent. In this case, we have always found the mean-field critical exponents and a slight deviation from them with the increasing degree-degree correlations. This mean-field behavior follows the predicted and observed critical behavior in other complex networks [13–17], in addition to being another agreement of what was conjectured by Grinstein *et al.* [24], i.e., we obtained the same universality class of the Ising model on a restricted scale-free network both in the equilibrium regime [16] as out of it.

-
- [1] J. W. Gibbs. Elementary Principles in Statistic Mechanics. (Yale Universality Press, New Haven, 1902);
- [2] T. Tomé and M. J. de Oliveira. Phys. Rev. A, 40, 6643 (1989);
- [3] T. Tomé, M. J. de Oliveira, and M. A. Santos. J. Phys. A: Math. Gen., 24, 3677 (1991);
- [4] R. Albert and A.-L. Barabási. Rev. Mod. Phys., 74, 47 (2002);
- [5] A.-L. Barabási and R. Albert. Science, 286, 509 (1999);
- [6] P. Erdős and A. Rényi. Mathematical Institute of the Hungarian Academy of Sciences, 5, 17 (1960);
- [7] D. J. Watts and S. H. Strogatz. Nature, 393, 440 (1998);
- [8] S. N. Dorogovtsev, A. V. Goltsev, and J. F. F. Mendes. Eur. Phys. J. B, 38, 177 (2004);
- [9] G. Bianconi and A.-L. Barabási. Phys. Rev. Lett., 86, 5632 (2001);
- [10] S. Aparicio, J. Villazón-Terrazas, and G. Álvarez. Entropy, 17, 5848 (2015);
- [11] A. L. M. Vilela, B. J. Zubillaga, C. Wang, M. Wang, R. Du, and H. E. Stanley. Sci. Rep., 10, 8255 (2020);
- [12] T. Gradowski and A. Krawiecki. A. Phys. Pol. A, 127, A-55 (2015);
- [13] S. N. Dorogovtsev, A. V. Goltsev, and J. F. F. Mendes. Phys. Rev. E, 66, 016104 (2002);
- [14] A. V. Goltsev, S. N. Dorogovtsev, and J. F. F. Mendes. Phys. Rev. E, 67, 026123 (2003);
- [15] R. A. Dumer and M. Godoy. Eur. Phys. J. B 95, 159 (2022);
- [16] R. A. Dumer and M. Godoy. Physica A, 612, 128795 (2023);
- [17] C. P. Herrero. Phys. Rev. E, 65, 066110 (2002);
- [18] C. P. Herrero. Phys. Rev. E, 69, 067109 (2004);
- [19] A. Aleksiejuk, J. A. Holyst, and D. Stauffer. Physica A, 310, 260 (2002);
- [20] G. Bianconi. Phys. Lett. A, 303, 166 (2002);
- [21] M. Leone, A. Vazquez, A. Vespignani, and R. Zecchina. Eur. Phys. J. B, 28, 191 (2002);
- [22] W. Figueredo and B. C. S. Grandi. Braz. J. Phys., 30, 58 (2000);
- [23] M. Godoy and W. Figueredo. Phys. Rev. E, 65, 026111 (2002);
- [24] G. Grinstein, C. Jayaprakash, and Yu He. Phys. Rev. Lett., 55, 2527 (1985);
- [25] W. Liu, W.-Y. Xiong, and J.-Y. Zhu. Phys. Rev. E, 71, 056123 (2005);

- [26] R. A. Dumer and M. Godoy. Phys. Rev. E, 107, 044115 (2023);
- [27] J.-Y. Zhu, W. Liu and H. Zhu. Eur. Phys. J. B, 33, 545 (2003);
- [28] H. Hong, M. Ha and H. Park. Phys. Rev. Lett., 98, 258701 (2007).
- [29] K. Binder and D. W. Heermann. *Monte Carlo Simulation in Statistical Physics. An Introduction*, 6rd ed. (Springer, Cham, Switzerland, 2019);
- [30] K. Binder and D. P. Landau. *A Guide to Monte Carlo Simulations in Statistical Physics*, 4rd ed. (TJ International Ltd, Padstow, UK, 2015);
- [31] L. Böttcher and H. J. Herrmann. *Computational Statistical Physics*, 1rd ed. (Cambridge University Press, NewYork, EUA, 2021);
- [32] S.-H. Tsai and S. R. Salinas. Braz. J. Phys., 28, 1, (1998);
- [33] M. E. J. Newman. Phys. Rev. Lett., 89, 208701 (2002);
- [34] F. W. S. Lima. Entropy, 18, 81 (2016);
- [35] A. L. M. Vilela, B. J. Zubillaga, C. Wang, M. Wang, R. Du, and H. E. Stanley. Sci. Rep., 10, 8255 (2020);